CHEMISTRY
A EUROPEAN JOURNAL

DOI: 10.1002/chem.200801458

Insights into Structure Direction of Microporous Aluminophosphates: Competition between Organic Molecules and Water

Luis Gómez-Hortigüela,*[a, b] Joaquín Pérez-Pariente,[a] and Furio Corà[b]

Abstract: A combination of experimental characterisation techniques and computational modelling has allowed us to gain insight into the molecular features governing structure direction in the synthesis of microporous aluminophosphates. The occlusion of three different structure-directing agents (SDAs), triethylamine (TEA), benzylpyrrolidine (BP) and (S)-(−)-*N*-benzylpyrrolidine-2-methanol (BPM), within the AFI structure during its crystallisation, together with the simultaneous incorporation of water, has been experimentally measured. We found a higher incorporation of organic molecules in the structure obtained with BPM, while a higher water (and lower organic) content is found for the ones obtained with TEA and BP as SDAs. The computational study provides a thermodynamic explanation for the observed behaviour in terms of the relative stabilisation energy of the SDAs and water molecules within the AFI framework compared with when they are in aqueous solution, and demonstrates that a competition for preferential occupation exists between water and organic SDAs, which is a function of the interaction with the inorganic framework. The lower interaction of TEA and BP molecules with the AFI structure promotes the simultaneous incorporation of water molecules in the 12-membered-ring (MR) channel, to increase the host–guest interaction energy and thus the thermodynamic stability. The presence of strongly interacting methanol groups in the BPM molecules leads to the incorporation of only organic molecules within the 12-MR channels. Our results demonstrate the essential role that water molecules play in the stabilisation of hydrophilic microporous aluminophosphates; a minimum amount of organic SDA is, however, essential for a templating role of the microporous architecture.

Keywords: molecular modeling · supramolecular chemistry · template synthesis · water chemistry · zeolites

Introduction

Since their discovery, crystalline microporous materials have found industrial application in processes such as catalysis, molecular sieving, gas separation and ion exchange,[1–3] which exploit the molecular dimensions and the crystalline nature of the microporous structure to discriminate between molecules with very subtle steric differences. Many different atoms can be incorporated within the oxide network of these crystalline microporous solids, thus giving rise to a range of materials with different compositions, several of which have useful catalytic properties. Since the discovery of microporous aluminophosphates ($AlPO_4$) by Wilson et al. in 1982,[4] the synthesis of these materials has been widely studied, yielding a diversity of structural types comparable to that of the previously known aluminosilicate-based zeolites.[5] In these $AlPO_4$ materials, there is strict alternation of Al^{3+} and P^{5+} ions; nevertheless, both ions can be isomorphically replaced by heteroatoms, which gives rise to acid, redox and even bifunctional properties. Known microporous $AlPO_4$ structures include polymorphs that are common to both SiO_2 and $AlPO_4$ compositions, but also structures that have no zeolitic counterpart.

These microporous oxides are synthesised through hydrothermal methods in which the source of the inorganic ions, water and, generally, an organic molecule, are heated in an autoclave for a time ranging from a few hours to weeks.[6–8] The inclusion of the organic molecules is usually required to direct the crystallisation of a certain microporous structure, and so they are called structure-directing agents (SDAs).

[a] Dr. L. Gómez-Hortigüela, Prof. J. Pérez-Pariente
Grupo de Tamices Moleculares
Instituto de Catálisis y Petroleoquímica—CSIC
C/Marie Curie 2, 28049 Cantoblanco, Madrid (Spain)
Fax: (+34) 91-585-4760
E-mail: lhortiguela@icp.csic.es

[b] Dr. L. Gómez-Hortigüela, Dr. F. Corà
Department of Chemistry, University College London
3rd floor, Kathleen Lonsdale Building, University College London
Gower Street, London WC1E 6BT (UK)

Supporting information for this article is available on the WWW under http://dx.doi.org/10.1002/chem.200801458.

The role of these organic molecules has been traditionally described as a "template effect"[9] to indicate that the organic molecules organise the inorganic tetrahedral units into a particular topology around themselves during the nucleation process, thus providing the initial building blocks from which crystallisation of the microporous structures will take place. Nevertheless, new theories are currently emerging[10–13] which suggest that the role that these molecules play during crystallisation of microporous materials is more complex than the one described in the initial template theory; the exact role of the SDAs is still far from being properly understood. Thus, the study of the structure-directing effect of organic molecules is a major issue in molecular sieves science. Controlling this feature would enable the synthesis of new topologies as well as the ability to gain control over crystal size and morphology and the location of heteroatoms, if present.

The organic SDA molecules are encapsulated within the nascent microporous structure during its crystallisation, developing strong non-bonded interactions with the framework and thus contributing to the final stability of the system. It is well known that microporous frameworks are metastable, and their intrinsic stability increases with the framework density, that is, denser materials are more stable than open frameworks. In this context, the organic molecules occluded within the void space of the open frameworks interact (through non-bonded interactions) with the surrounding oxide network, providing in this way the required thermodynamic stabilisation to make viable the crystallisation of open structures. Therefore, the SDA molecules template the crystallisation of the microporous frameworks by being occluded inside the pores, and also alter the relative thermodynamic stability of different framework structures through the different SDA–framework interaction energies.

Despite the large number of studies about the role of these organic molecules in the crystallisation of microporous materials, there is another important component in the synthesis gel that has attracted less attention, namely the water molecules. Water is present during the synthesis of both pure-silica and aluminophosphate microporous frameworks, and it does indeed influence the crystallisation mechanism.[10–13] With regard to the incorporation of water in the void space of the microporous structures, silica-based microporous materials do not usually occlude water molecules due to the hydrophobic character of the SiO_2 network. However, the higher hydrophilicity of $AlPO_4$-based networks, which comes from their molecular-ionic nature, with a strict alternation of Al^{3+} and P^{5+} ions in the oxide network, allows them to incorporate water molecules inside their structure during crystallisation, thus developing strong interactions.

The sorption and structure of water molecules in calcined microporous aluminophosphates have been widely studied;[14–16] it was found that water molecules adopt interesting helicoidal structures with double (in AlPO-5[17]) or triple (in VPI-5[18,19]) water helices, stabilised by H-bond networks. However, these structural studies usually considered adsorption of water in the structures in post-synthetic steps (after calcination of the SDA molecules used to obtain the microporous material). To our knowledge, no systematic studies of the structure-directing role that water molecules might play during the crystallisation of microporous frameworks have yet been performed. Thus, in the present work we aim to characterise the role that water molecules play in the structure direction of hydrophilic microporous aluminophosphates, in addition to the usual organic SDA molecules.

Three organic molecules with different shape, size, hydrophilicity and chemical properties, namely triethylamine (TEA), benzylpyrrolidine (BP) and (*S*)-(−)-*N*-benzylpyrrolidine-2-methanol (BPM) (Figure 1, bottom), were studied as

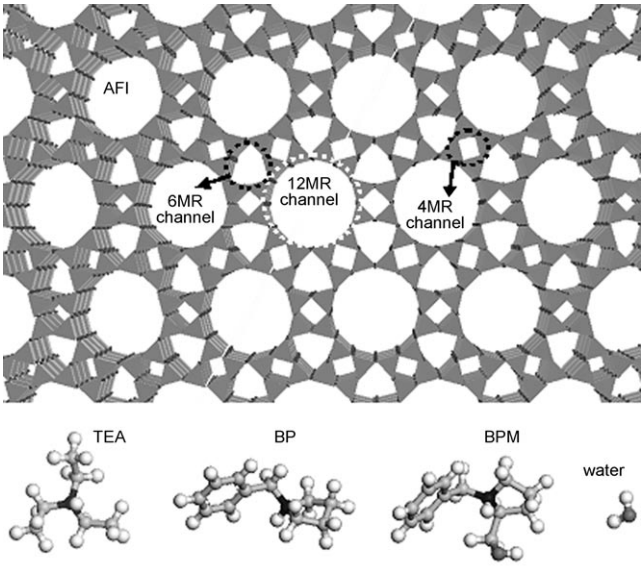

Figure 1. Top: AFI structure, viewed perpendicularly to the channel direction, which shows the different channels. Bottom: Molecular structures of TEA, BP, BPM and water. Nitrogen, oxygen and carbon atoms are displayed in black, dark grey and light grey, respectively.

SDAs for the synthesis of the AlPO-5 microporous material (AFI-type structure). The AFI structure is composed of one-dimensional 12-membered-ring (MR) channels with a diameter of 7.3 Å, which are surrounded by smaller one-dimensional 4- and 6-MR channels,[5] as illustrated in Figure 1 (top). Our work consisted in the synthesis and experimental characterisation of the different samples to determine experimentally the organic and water content in each case, and a subsequent computational study in an attempt to understand the energetics governing the incorporation of organic SDAs and water molecules.

Computational Methodology

A computational study was performed to understand the energetics involved in the occlusion of the organic molecules and water within the AFI structure during crystallisation.

General details of the computational work are given in the Experimental Section. Although the computational models to simulate SDA occlusion in nanoporous frameworks are now well established, an ability to account for competition of the SDAs with water is a new extension that we propose herein for the first time. In this section, we explain the choice of the computational models we have developed and applied to this goal.

Computational protocol: Our main aim in the computational study was to identify whether water molecules from the solvent of the synthesis gel have any primary role in the structure direction. In the case of the AFI structure considered here, the 12-MR channels are the only cavities large enough to accommodate the organic molecules. We shall therefore be concerned with whether water molecules can be occluded in these 12-MR pores as an alternative or in addition to the organic SDAs, to indicate the presence of competition or cooperativity between water and organic SDAs in structure direction.

A minimum number of organic SDA molecules are required to stabilise the microporous framework architecture; synthesis from water solutions without SDAs does in fact yield dense architectures, such as AlPO-C or trydimite. Although competition between water and SDA may exist, we can clearly identify a primary molecule, the organic SDA, and a secondary one, water, in the space-filling effect. The two can, however, contribute in a different ratio to the pore filling; the problem should therefore be addressed computationally as an open system in which the optimal number of water and SDA molecules per unit cell of the host framework has to be addressed simultaneously.

To find a general solution to this problem we have defined the following protocol:

1) First, maximum loading of the primary space-filling molecule, the organic SDA in this case, is determined by Monte Carlo (MC) docking simulations.
2) From the maximum value obtained above, the number of primary SDA molecules is decreased in discrete steps until large sections of empty space appear in the structure. The location of the SDAs is obtained by simulated annealing and energy minimisation calculations.
3) For each content of primary SDA investigated, the incorporation of water is studied by a second MC docking step, followed by simulated annealing and energy minimisation steps to evaluate the final geometry and interaction energies.

The steps listed above enable us to estimate the total internal energy of the system as a function of the ratio between SDA and water molecules inside the microporous framework. Under thermodynamic control, the number of SDA and water molecules per unit cell will be that corresponding to the global minimum in this energy curve. From the shape of this energy curve, for example the presence of multiple minima, we can determine whether there is a competition or a cooperative effect between water and the organic SDAs for the adsorption sites within the micropores. The computational work can further shed light on the relative contribution of water and SDAs to the thermodynamic stability of the system.

The stabilisation provided by the occlusion of the different molecules, SDAs and water, comes from the interaction between these species themselves and with the microporous network. In a true synthesis of a nanoporous solid, SDA and water molecules do not come from a vacuum but from the synthesis gel, which is in practice a concentrated solution of the relevant species. To obtain a realistic computational approximation to the true thermodynamics of the synthesis, we also have to take into account the relative stability of the SDA and water molecules in the synthesis gel. In our work, we represented the sources of water and SDAs, respectively, as liquid water and a water solution containing the SDA cations at the same concentration as that employed experimentally. The net stabilisation provided by the occlusion of SDAs and water within the AFI framework will be given by the interaction energy (defined as the final energy of the whole system minus the energy of the molecules in vacuo) minus the energy of the species in the water solution. Hence, the net stabilisation energies will be obtained by the following expression [Eq. 1]:

$$\Delta E = [E_f - (n_{SDA} \cdot E_{SDA\ in\ vacuo} + n_{H_2O} \cdot E_{H_2O\ in\ vacuo})] - [n_{SDA} \cdot E_{hyd\ SDA} + n_{H_2O} \cdot E_{vap\ H_2O}] \quad (1)$$

where E_f refers to the final internal energy (per unit cell) of the AFI system containing SDA and water molecules, n_{SDA} and n_{H_2O} are the number of SDA and water molecules per unit cell of AFI, respectively, $E_{SDA\ in\ vacuo}$ and $E_{H_2O\ in\ vacuo}$ are the energies of the molecules optimised in vacuo, $E_{hyd\ SDA}$ is the hydration energy of the corresponding SDA and $E_{vap\ H_2O}$ is the vapourisation energy of water. The terms in the second square bracket of Equation (1) account for the energetic cost of transferring water and SDA molecules from the aqueous solution to the AFI framework. By including these terms, we can estimate the most stable loading ratio of SDA and water molecules within the AFI framework in equilibrium with their aqueous solution. Details of the simulations of the liquid phases are given below.

Vapourisation energy of water and hydration energies of the SDAs: The vapourisation energy of liquid water was calculated by generating a system containing 80 water molecules described under periodic boundary conditions (PBCs). The system was equilibrated by running 500 ps of molecular dynamics (MD) at 300 K in the constant normal pressure and temperature (NPT) ensemble. Then, the five configurations with the lowest energies were extracted from the MD trajectory and energy minimised, from which the lowest value of the internal energy was taken. The vapourisation energy was then calculated by subtracting the energy of the water molecules in vacuo, and normalising to one water molecule. This calculation resulted in a vapourisation energy of

$-12.40\,\mathrm{kcal\,mol^{-1}}$, which represents the energetic cost to remove a single water molecule from the aqueous solution. This value is in reasonably good agreement with the experimental value of $-10.77\,\mathrm{kcal\,mol^{-1}}$.[20]

The hydration energy of the different SDA molecules was calculated by generating a box containing 80 water and two organic SDA molecules under PBCs; this value reproduces computationally the same SDA concentration as in the synthesis gel (1 SDA:40 H_2O). The insertion of two independent SDA molecules in the simulations enables us to include SDA–SDA interactions in the gels. This is particularly important for BP and BPM, which have been shown in our previous work to exhibit supramolecular chemistry leading to the formation of molecular dimers. Due to the high pH of the synthesis gels ($\approx$3), protonated SDA molecules were studied; the +1 charge of the SDA molecules was compensated by decreasing the oxygen charge in each water molecule until charge neutrality was achieved. This is the same method employed here to achieve charge balance upon inclusion of the SDAs in the AFI framework, and ensures internal consistency of the results. These SDA solutions were equilibrated by running 500 ps of NPT MD at 300 K, then the five configurations with the lowest energies were extracted and energy minimised, and the lowest value of the internal energy was taken as the total solution energy (E_{sol}). The hydration energy was calculated according to Equation (2):

$$E_{\mathrm{hyd\,SDA}} = {}^1\!/_2(E_{\mathrm{sol}} - 80 \cdot E_{\mathrm{vapouris\,H_2O}} - 2 \cdot E_{\mathrm{SDA\,in\,vacuo}}) \qquad (2)$$

In this way, the hydration energies were calculated as -82.84, -90.21 and $-91.61\,\mathrm{kcal\,mol^{-1}}$ for TEA, BP and BPM, respectively.

Simultaneous occlusion of SDAs and water inside the AFI structure: Following the previously detailed protocol, the first step in our calculations was to study the maximum number of SDA molecules that the AFI structure can host; these values were obtained through MC simulations and were found to be two TEA, 1.33 BP and 1.33 BPM molecules per unit cell (the last two in the dimer configuration, as will be explained below). Nevertheless, to know the energetic cost of reaching higher loadings and thus complete the profile of the energy curve, higher packing values (2.5 for TEA and 1.5 for BP and BPM) were also studied by manually inserting the additional molecules.

Next, different contents of the three organic molecules in the AFI structure were studied. For TEA molecules, six packing values of 2.5, 2.0, 1.5, 1.25, 1.0 and 0.75 molecules per unit cell were studied. In the AFI structure, each 12-MR channel can be considered to be isolated from the rest of the 12-MR channels because they are one-dimensional in nature, and thus not interconnected. Therefore, AFI supercells with different sizes along the 12-MR channel (unit cells along the *c* direction) were employed to achieve the different loadings of organic molecules listed above. Packing values of 2.5, 2.0, 1.5 and 1.0 were studied by loading five, four, three and two TEA molecules in a $1\times1\times2$ supercell of the AFI system, respectively, whereas values of 1.25 and 0.75 were studied by loading five and three TEA molecules in a $1\times1\times4$ supercell. For BP and BPM, the asymmetric nature of the molecules enables two different relative orientations between adjacent molecules: with benzyl rings on opposite sides (opp) or facing each other (same side, ss) (see Figure 7 top and bottom, respectively). The packing value of 1.33 is reached when rings are located parallel to each other to form dimers (see Figure 7, bottom), as we have already demonstrated.[21–23] This arrangement was studied for BP by loading four BP molecules (arranged as dimers, ss) in a $1\times1\times3$ unit cell system, whereas for BPM, 24 BPM molecules were loaded in a $1\times1\times18$ unit cell system (for details of these systems, see refs. [21,23]). The very large cell in the latter case is required to enable the stable relative orientation between adjacent dimers, which is long-range ordered, as described in ref. [23]. This packing value was also studied for the "opp" configuration by loading four BP or BPM molecules in a $1\times1\times3$ unit cell system. Higher loadings of 1.5 were studied by manually loading (as MC simulations did not reach such a high organic content) six BP or BPM molecules (in the required orientation) in a $1\times1\times4$ AFI supercell. Packing values of 1.2 and 0.8 were studied by loading six and four organic molecules in the required orientation in a $1\times1\times5$ supercell, whereas values of 1.0 were studied by loading four molecules in a $1\times1\times4$ supercell system of the AFI framework; the packing value of 0.66 was studied by loading two molecules in a $1\times1\times3$ supercell. For BP, additional values of 1.11 and 0.89 were studied by loading ten and eight BP molecules, respectively, in the required orientation in a $1\times1\times9$ AFI supercell. For each loading, the most stable location of the organic molecules (initially without water) was found by running five cycles of simulated annealing calculations, and the most stable configuration was taken for subsequent calculations with water.

Water molecules were then inserted in the organic-containing AFI systems through grand canonical (*pvT* ensemble) MC simulations, in which Coulomb interactions were explicitly included. A constant water partial pressure of 1000 kPa was used; this high pressure was selected to ensure the full loading of water and to accelerate the loading convergence. Such a high partial pressure is, however, not unrealistic for hydrothermal synthesis conditions. A total of 2.5 million configurations were sampled, thus ensuring that the loading of water molecules had reached equilibrium. Then, the location of both water and organic SDA molecules and the final internal energies (E_f) for each system were obtained by running ten cycles of simulated annealing calculations. These final energies, together with the solution values described earlier, were employed to calculate the net stabilisation energies for each system by using Equation (1).

Results

Experimental results: Despite the different molecular structures of the three SDAs examined here, the XRD patterns of the samples indicated that the three molecules directed the synthesis of the AFI structure without impurities (see Figure 1 in the Supporting Information). The organic content of the molecules, as measured by elemental analysis, is shown in Table 1. The C/N ratio observed was very close to the theoretical value, which evidenced the resistance of the molecules to the hydrothermal treatment and their integral incorporation within the AFI structure. The incorporation of the organic molecules was observed to increase from TEA (6.66±0.02%) to BP (9.29±0.10%) and BPM (13.24±0.07%), resulting in values of packing of 1.13, 1.00 and 1.23 (±0.01) organic molecules per AFI unit cell, respectively.

Table 1. Elemental CHN analysis of the AlPO-5 samples.

Sample	% C	% H	% N	C/N[a]	% organic[b]	H_2O per unit cell
TEA	4.70	1.95	1.08	5.1 (6)	6.66 (1.13)	7.72
BP	7.57	1.21	0.71	12.4 (11)	9.29 (1.00)	5.64
BPM	9.93	1.56	1.09	10.7 (12)	13.24 (1.23)	3.83

[a] Theoretical C/N value in parentheses. [b] Organic molecules per unit cell in parentheses.

The thermogravimetric analysis (TGA) results (in air) are shown in Figure 2. A very strong desorption at temperatures below 125°C can be clearly observed for the AFI sample obtained with TEA as the SDA, which might correspond to the release of water. In addition, another strong desorption can be observed in the 125–250°C range, followed by weaker desorptions at higher temperatures (up to 600°C), the latter probably due to combustion of the remaining TEA. In the sample obtained with BP, a strong desorption is also observed at temperatures below 220°C that might correspond to desorption of water, whereas desorption and combustion of the organic molecules occur at higher temperatures from 250 up to 700°C. Finally, the AFI sample obtained with BPM shows a much less intense desorption at temperatures below 220°C, which suggests a lower water content, whereas the desorption at temperatures higher than 220°C is more intense than in the previous cases. This result is in agreement with the higher organic content observed for BPM from elemental analysis.

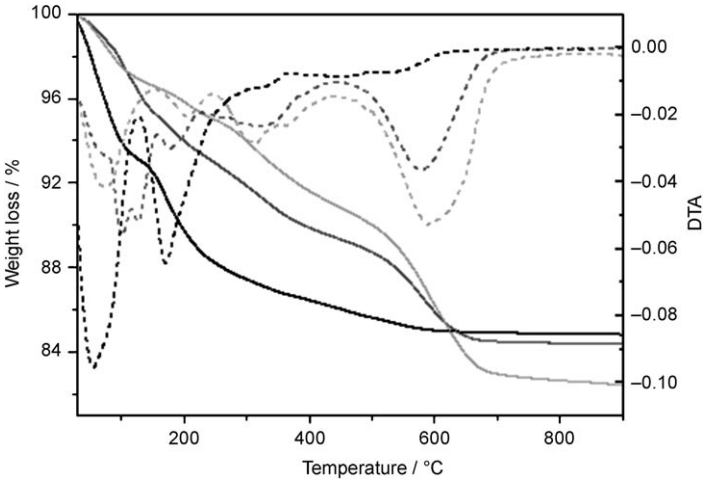

Figure 2. TGA (——) and differential thermal analysis (DTA) (-----) of AlPO-5 samples in air. (AlPO-5-TEA: black lines, AlPO-5-BP: dark grey lines, AlPO-5-BPM: light grey lines)

In the AlPO-5–TEA sample it is not clear whether the desorption at low temperatures (below 300°C) corresponds to the release of water, of the organic molecules or the simultaneous desorption of both species. To shed further light on the nature of the species desorbed in this temperature range, TGA coupled with mass spectrometry was performed under a helium atmosphere to chemically analyse the evolved gases. The results for TEA and BP are shown in Figure 3 (the results for BPM are similar to those for BP).

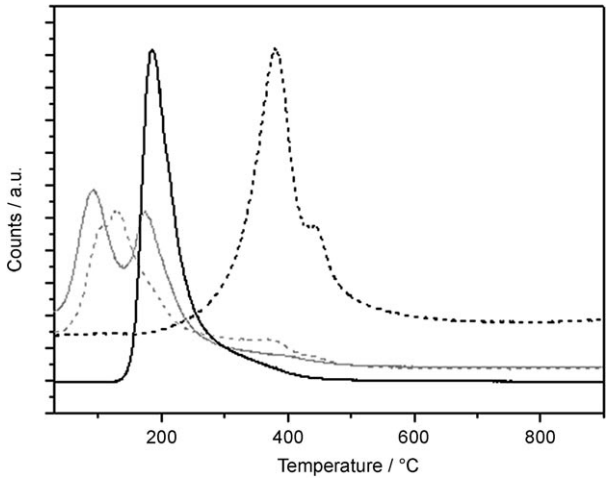

Figure 3. TGA mass of AlPO-5 samples obtained with TEA (——) and BP (-----) in helium. Desorption of water (monitored by m/z 18) is displayed in grey and desorption of the organic molecules (monitored by m/z 86 for TEA and 91 for BP, respectively) is displayed in black.

In the sample obtained with BP, it can be clearly observed that the desorption of water and organic SDAs does not overlap: water is released at temperatures below 220°C whereas BP is desorbed at temperatures above 220°C, with a maximum desorption rate at about 400°C. The same occurs for the desorption of BPM, which starts at temperatures above 220°C, and thus the observed desorption at lower temperatures will correspond exclusively to the release of water. However, a different picture is observed for the sample obtained with TEA as SDA. In this case, two clear water desorptions can be observed, one at temperatures around 100°C and another that occurs simultaneously with the desorption of the organic TEA molecule at temperatures around 175°C. This result indicates that the desorption of TEA from the AFI channels is accompanied by a simultaneous release of water.

The previous results allowed us to estimate the water content of the different samples from TGA performed in air (carried out under the same humidity conditions). The amount of loaded water was calculated by subtracting from the total weight loss the weight loss corresponding to the organic content (calculated from the elemental analysis) and the weight loss corresponding to the loss of hydroxyl groups present in the AFI structure (calculated from the TGA results of the calcined sample). In this way, 7.72, 5.64 and 3.83 water molecules were occluded within the AFI structure obtained by using TEA, BP or BPM as SDA, respectively.

As a summary, 1.13 TEA (6.66%) and 7.72 water molecules are occluded in the AlPO-5 as-made sample obtained by using TEA as SDA, whereas 1.00 BP (9.29%) and 5.64 water molecules are occluded when BP is used, and finally 1.23 BPM (13.24%) and 3.83 water molecules when BPM is the SDA. If we compare the amount of organic occluded (in percentage, due to the different molecular size), it can be clearly observed that the higher the organic occlusion, the lower the water loading. This result suggests that the space within the AFI framework that is not filled by the organic SDAs is occupied by water molecules, which indicates that competition or cooperation of the two species may exist.

Table 2. Stabilisation energies (S.E.) of the molecules with different packing values, given in kcal mol^{-1} per AFI unit cell. SDA and water contents are given per unit cell. Water content is given as the sum of water in the 6-MR channels plus the 12-MR channels. The most stable packing values are highlighted in bold. Higher organic contents than those found by MC simulations are highlighted in italic.

SDA	Packing (SDA)	Water content	S.E.	SDA	Packing (SDA)	Water content	S.E.
TEA	0.75	4+8.5	−45.1	BP	0.6-ss	4+8	−47.1
	1	**4+6.5**	**−53.4**		0.6-opp	4+9	−50.7
	1.25	4+5	−53.1		0.8-ss	4+5.4	−43.7
	1.5	4+3	−47.7		0.8-opp	4+6.4	−46.5
	2	4+0	−40.7		0.9-ss	4+4.8	−44.8
	2.5	*4+0*	*46.4*		0.9-opp	4+5	−46.6
BPM	0.6-ss	4+7	−55.1		1-ss	4+5	−49.7
	0.6-opp	4+7	−53.2		**1-opp**	**4+5.3**	**−53.1**
	0.8-ss	4+5.4	−49.0		1.1-ss	4+2.3	−50.2
	0.8-opp	4+5	−46.2		1.1-opp	4+2.9	−52.4
	1-ss	4+3.5	−50.8		1.2-ss	4+1.6	−46.2
	1-opp	4+2.5	−49.0		1.2-opp	4+1.6	−45.6
	1.2-ss	4+1.2	−56.9		**1.3-ss**	**4+0**	**−53.7**
	1.2-opp	4+1	−49.5		1.3-opp	4+0	−51.0
	1.3-ss	**4+0**	**−66.9**		*1.5-ss*	*4+0*	*−37.1*
	1.3-opp	4+0	−53.8		*1.5-opp*	*4+0*	*−42.2*
	1.5-ss	*4+0*	*−29.3*	H_2O	H_2O	4+15	−27.5
	1.5-opp	*4+0*	*−18.8*				

Computational results: The computational study was performed in an attempt to explain the experimental results regarding the different organic and water contents found for the three systems; in doing so, we also aim to provide an understanding of the molecular features that govern the structure direction of these molecules in the synthesis of microporous aluminophosphates. For every molecule and packing value (organic content), our set of calculations allowed us to determine the maximum amount of water that could be occluded within the AFI framework, and the stabilisation energy of the corresponding system. Energetic results are summarised in Table 2 and Figure 4.

Occlusion of water in the 6-MR channels: Before discussing the occlusion of water in the 12-MR channels where SDAs also reside, we note that water can be incorporated in the side 6-MR channels of the AFI structure, as depicted in Figure 5. Such channels can host four water molecules per unit cell, which originate strong electrostatic interactions with the oxide network of the AFI framework. This water–6-MR channel interaction accounts for about 15–20% of the total interaction energy developed in the systems, and provides direct evidence that occluded water plays an important role in the energetic balance of the synthesis and stabilises the nanoporous materials during crystallisation. Indeed, a close relationship between the molecular size and geometry of the water molecules and those of the 6-MR channels can be observed (Figure 5), which suggests a possible templating role of water in the formation of such small channels.

Importantly, all the water molecules within the 6-MR channels are always oriented in the same direction (see Figure 5, bottom), with hydrogen atoms pointing towards the Al ions composing the Al–O–P bonds that run parallel to the channel direction. Klap et al. have shown in a series of papers[24–26] that the Al–O–P vector (of the T–O–T bonds parallel to *c*) always points in the same direction (in fact, AFI crystal growth only takes place in that direction), thus giving a permanent polarisation to the crystal along the *c* direction. This macroscopic polarisation may cause the alignment of the water molecules in the 6-MR channels.

Occlusion of TEA: Docking of TEA molecules in the AFI framework shows that the maximum loading corresponds to 2.0 molecules per unit cell, although only 1.13 were found experimentally. A range of organic contents between 0.75 and 2.5 molecules per unit cell, with simultaneous occlusion of water, was then studied computationally; when the number of TEA molecules is less than 2.0 per unit cell, empty space is available in the 12-MR channels of the structure to enable incorporation of water. Our results show that 8.5 (34 in the $1\times1\times4$ supercell), 6.5 (13 in the $1\times1\times2$ supercell), 5 (20 in the $1\times1\times4$ supercell), 3 (6 in the $1\times1\times2$ supercell) and 0 water molecules per unit cell were loaded in the 12-MR channel for organic contents of 0.75, 1.0, 1.25, 1.5 and 2.0 TEA molecules per unit cell, respectively, in addition to the four water molecules per unit cell loaded in the 6-MR channels. A clear separation of water and organic phases occurred for a TEA packing value of 0.75, for which we observed the formation of hexamer- and double hexamer-shaped water ring-clusters between TEA molecules (see Figure 6, top), which reveals a physical separation of the species in different phases. This separation is due to the low loading of organic molecules and, consequently, the large water to SDA ratio, which prevents a cooperative effect in the structure direction. Hence, no packing values lower than 0.75 were studied. Packing values equal to or

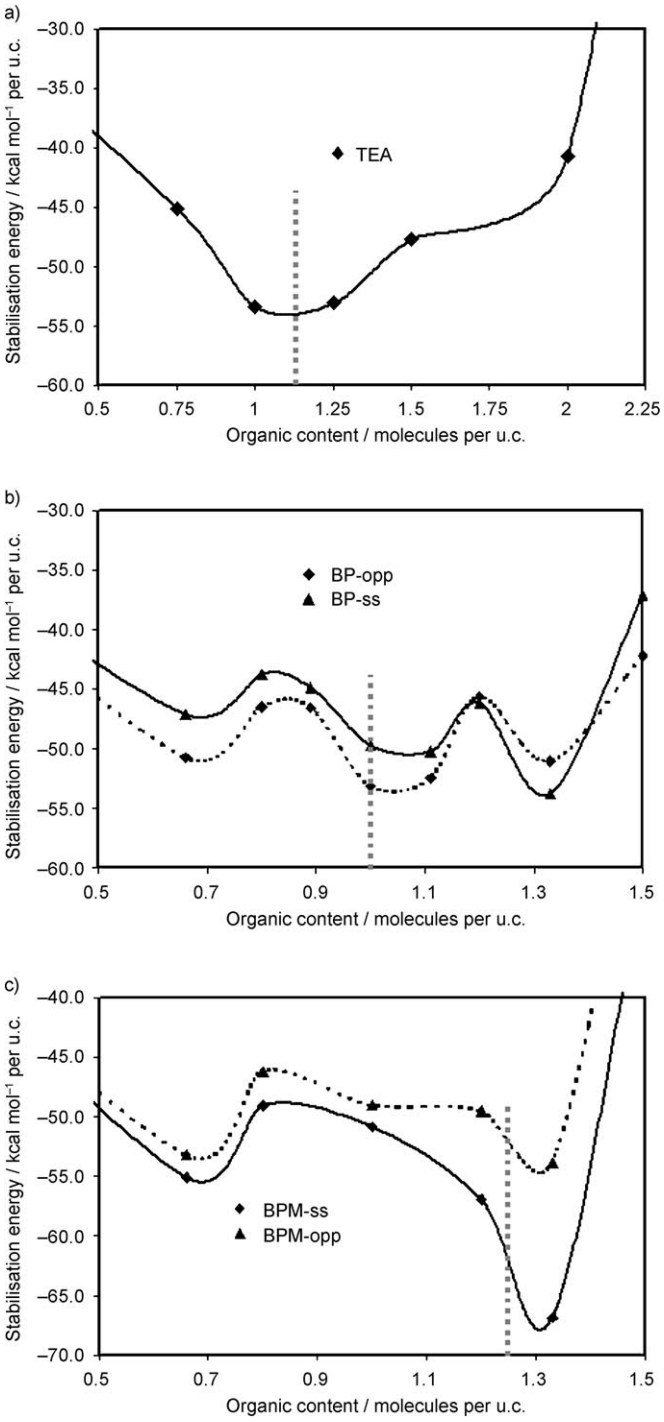

Figure 4. Stabilisation energy of the different systems studied as a function of the organic content: a) TEA, b) BP and c) BPM. In the BP and BPM systems, the two orientations are distinguished as solid lines (ss: benzyl rings facing each other) and dashed lines (opp: benzyl rings on opposite sides). All the energies are given in kcal mol^{-1} per unit cell. The organic content found experimentally is shown by the vertical dashed line.

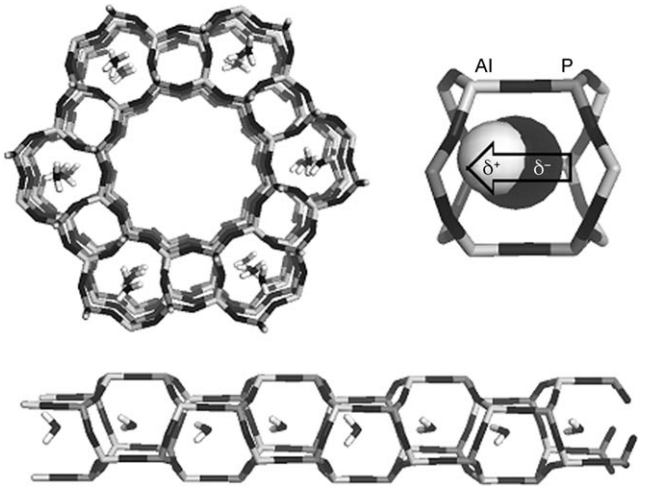

Figure 5. Location of water molecules within the 6-MR channels of the AFI structure. Top left: view perpendicular to the channel direction; top right: filling of water molecule in the 6-MR channel. Bottom: orientation of water molecules inside the 6-MR channel. Al, P, O and H atoms are displayed in light grey, dark grey, black and white, respectively.

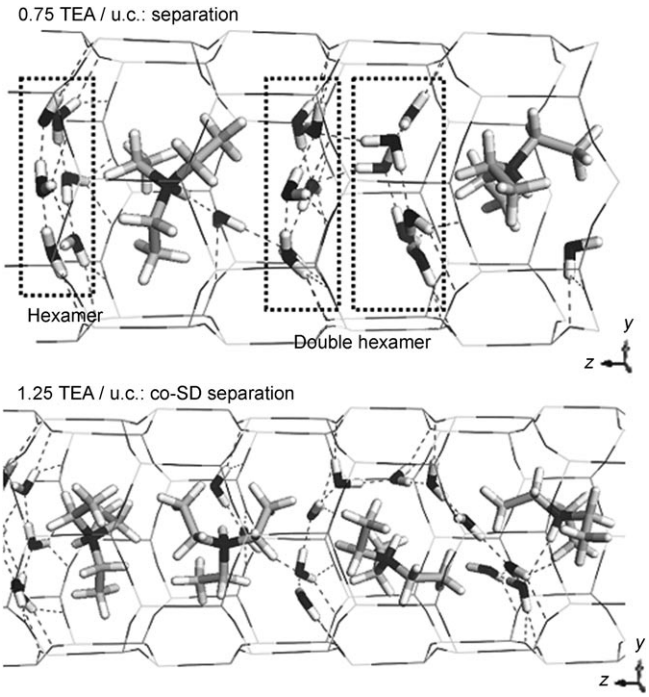

Figure 6. Water clusters formed between the organic TEA molecules. Top: physical separation of phases in the AFI framework loaded with 0.75 TEA molecules per unit cell (u.c.); single (left) and double (right) water hexamers are formed between the organic molecules. Bottom: co-structure-directing (co-SD) effect of TEA and water molecules in the AFI framework loaded with 1.25 TEA molecules per unit cell, which shows the water chains surrounding the organic molecules. Dashed lines indicate the H-bond network. N, O and C atoms are displayed in dark grey, black and light grey, respectively.

higher than one TEA molecule per unit cell did not lead to such separation; in this case, water molecules were mostly arranged as H-bonded water chains surrounding the organic molecules (see Figure 6, bottom), which reveals a close interaction of water and SDAs and thus a possible cooperative structure-directing effect during the AFI crystallisation.

The energy results (shown in Figure 4) indicate that the systems where 1 and 1.25 TEA molecules (6.5 and 5 water molecules) per unit cell are occluded in the 12-MR channels (10.5 and 9 water molecules when water in the 6-MR channels is included) are the most stable ones; this result is in very good agreement with the experimental value found of 1.13 TEA molecules. The location of the molecules for an organic content of 1.25 TEA is shown in Figure 6 (bottom): water molecules form chain clusters around the TEA molecules, which suggests a co-structure-directing effect (TEA and water) in the synthesis of the AFI structure. The energy decomposition in the different contributions (Table 1 in the Supporting Information) indicates that the interaction between the SDAs and the AFI framework for the most stable SDA contents (1 and 1.25) contributes to approximately half of the total interaction energy, while the other half comes from water–AFI and water–SDA interactions.

As a further measure of the structure-directing ability, the space-filling efficiency of the SDA and water species within the 12-MR channel in each system was estimated by measuring the free volume space from the van der Waals surfaces. It was found that the best space filling (the lowest free volume available) is achieved when the 12-MR channel is loaded exclusively with TEA molecules, although it does not lead to the highest thermodynamic stability (see Table 1 in the Supporting Information).

Occlusion of BP: The maximum organic content that the AFI structure can host is 1.33 BP molecules per unit cell, whereas the experimental value found was 1.00. Packing values of 1.5, 1.33, 1.2, 1.11, 1.0, 0.89, 0.8 and 0.66 BP molecules per unit cell were studied. In addition, two different orientations between the organic molecules were tried for each packing value, with benzyl rings on opposite sides ("opp") or on the same side (facing each other: "ss").

The results for water loadings are shown in Table 2. The larger size of BP relative to TEA causes a lower water inclusion for the same organic content (in molecules per unit cell). Again, the lowest organic content studied in our work (0.66 molecules per unit cell) led to a physical separation of water and SDA molecules owing to the high water content (more than 12 water molecules per BP in the 12-MR channel): several water ring-clusters were found between the organic molecules. Organic contents higher than 0.8 molecules per unit cell did not lead to such separation; in these cases, water molecules formed chain clusters around the organic molecules (see Figure 7, top).

The energy results (Figure 4, middle) showed the presence of several local minima in the stabilisation energy curve, whose value further depends on the relative orientation (opp/ss) of the SDA molecules. When benzyl rings were on opposite sides, the best packing value was about 1 BP and 5.3 water molecules (9.3 when water in the 6-MR channels is included) within the AFI framework (Figure 7, top), whereas facing benzyl rings led to a most stable organic content of 1.33, that is, the dimer configuration, and 0 water molecules (4 when water in the 6-MR channels is included).

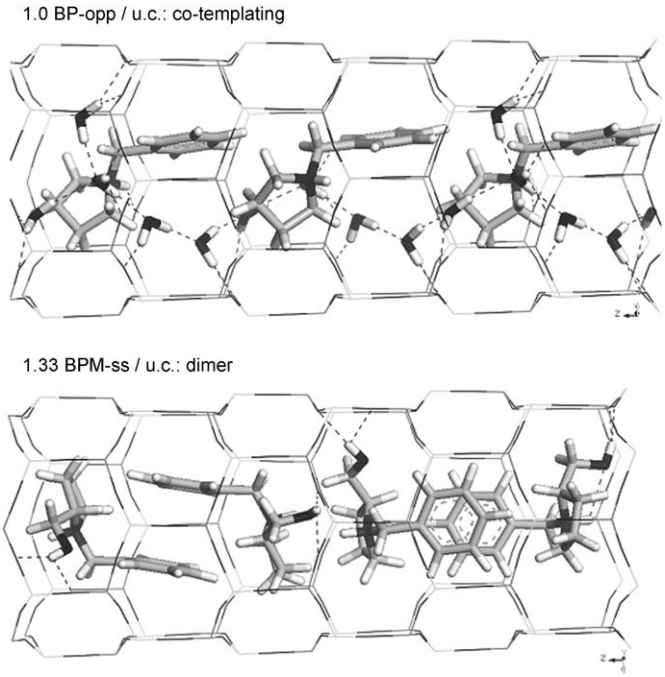

Figure 7. Top: stable configuration for BP, with one organic molecule (in "opp" configuration) and 5.3 water molecules per unit cell in the 12-MR channel. Bottom: the most stable configuration for BPM, with 1.33 organic molecules per unit cell in the dimer configuration and no water in the 12-MR channel. N, O and C atoms are displayed in dark grey, black and light grey, respectively.

The energies of these two configurations are very similar, and it may be argued that both situations are expected to occur. In addition, for the "opp" configuration, another local minimum was found for a packing value of 0.66 molecules per unit cell (with 13 water molecules in total), although in this case there was a clear physical separation of water and organic molecules. The energy differences found for this system suggest the preferential occurrence of this competing SDA/water content in the AFI structure, which corresponds to 1.0 (and 9.3 water molecules) or 1.33 BP molecules (and 4 water molecules), although packing of 0.66 BP (and 13 water molecules) could also be present in a minor concentration. This result is again in good agreement with the experimental value of 1.00 BP molecules, which is close to a weighed average of the three minima. The existence of these three minima with different SDA/water ratios with similar stabilities suggests a competition between the organic and water molecules to enter the AFI structure during crystallisation. In addition, the energy results demonstrate that the "opp" configuration is more stable than the "ss" one, except at the high loading of 1.33, when closely packed "ss" BP dimers are stable.

The free volumes calculated for this system evidenced a higher efficiency in space filling for the system with the most stable packing, that is, 1 BP (in the "opp" configuration), which may explain at least in part its higher stability.

Occlusion of BPM: In this case, the same two molecular configurations ("ss" and "opp") already discussed for BP and organic contents of 1.5, 1.33, 1.2, 1.0, 0.8 and 0.66 BPM molecules per unit cell were studied. The results for the water contents are shown in Table 2. A lower inclusion of water in the 12-MR channels is found in this system with respect to the one with BP, caused by the higher molecular size of BPM owing to the presence of the methanol group. As in the previous case, a packing value of 0.66 BPM molecules per unit cell led to such a high water content that the physical separation of SDA and water phases occurred (more than ten water molecules per BPM molecule were occluded in the 12-MR channel).

In contrast with the BP case, a clear energy minimum is found for the highest organic content (Figure 4, bottom), with the molecules arranged in the dimer configuration ("ss", 1.33 molecules per unit cell: Figure 7, bottom). Under these conditions, the efficient space-filling ability of the BPM molecules prevented any incorporation of water molecules in the 12-MR channel (only four water molecules are occluded in the 6-MR channels). Interestingly, such increased stability for the highest organic content found in the simulation is again in good agreement with the experimental findings, in which 1.23 BPM molecules per AFI unit cell were occluded.

The free volumes calculated showed more efficient space filling when the system is exclusively loaded with organic molecules, in agreement with its higher stability.

Occlusion of only water in the 12-MR channels: For completeness, the AFI system in which only water molecules were loaded was also studied. In this case, the computational results showed that 15 water molecules were occluded within the 12-MR channel of the AFI framework (19 when water in the 6-MR channels is included), and developed a stabilisation energy of $-27.5\,\mathrm{kcal\,mol^{-1}}$ per unit cell. This water content is very similar to that found experimentally in a calcined AFI sample after hydration, which was calculated by TGA (Figure 2 in the Supporting Information) to be 18 water molecules per unit cell. The close proximity of these water contents gives further confidence to our simulation results for the study of water and SDA occlusion.

Discussion

Our results demonstrate that the internal space of microporous frameworks during the synthesis is not exclusively occupied by the organic SDA molecules, and that water can play a primary role in structure direction. The structure-directing effect is therefore more complex than originally envisaged.

A close examination of the curves of Figure 4 shows that three distinct situations may occur. First, the curve displays a single minimum as a function of the SDA/water ratio, as exemplified by BPM, and this minimum corresponds to a zero water content (at least in the channel where the SDAs reside). This case represents a synthesis in which structure direction is due uniquely to the organic SDA, and water only plays a passive role of solvent for the synthesis reaction (apart from its occlusion in the side 6-MR channels). Second, the curve displays a single minimum, but this occurs for a non-zero water content, as exemplified here by TEA. In this situation water acts necessarily as a solvent but also has a primary structure-directing role, and the true structure-directing species is not the organic SDA itself but an aggregate between SDA and water. We define this situation as cooperative structure direction; water is required to achieve the thermodynamically stable composition of the system. In the third case, exemplified by BP, multiple minima of comparable energy are clearly present in the thermodynamical stability, and correspond to different SDA/water ratios. This case is representative of a competition between the organic SDA and water for the available internal space of the microporous host. In the latter case, water again plays an active role in the synthesis. Such a distinction of the role of water can only be defined by examining the systems at different SDA/water loadings; the concepts of competition or cooperativity between water and SDAs have a natural definition linked to the shape of the energy surface as a function of the SDA/water ratio. Having available a calculated energy curve of the type shown in Figure 4 therefore enables us to widen our description and understanding of structure direction.

The computational findings are in good agreement with the experimental observations, both regarding the relative water and organic contents of the different systems and the most stable loading for each SDA molecule. A slightly higher water content is found in the simulations compared with the value experimentally measured from TGA of the as-made samples. This difference can be explained by the different conditions that exist during crystallisation of the AFI structure and post-synthetic characterisation (TGA): the water pressure at which the AFI structure is crystallised inside the autoclave is much higher than that at which the TGA of the as-made samples are performed, and therefore the water content of the crystallising AFI structure during hydrothermal synthesis might be higher than when TGA is performed, which would be in agreement with the computational findings. It should be mentioned here that possible errors coming from the approximations assumed by using molecular mechanics methods would be systematic for all the systems, and so they would cancel out when examining trends. In fact, the good comparison of our simulation study with the experimental results gives confidence in the simulation model we have employed, and indicates that our model accounts properly for the main factors that govern the incorporation of organic and water molecules within the AFI structure, including both space-filling effects and stabilisation energies.

When TEA is used as the SDA, although the AFI topology can host as many as two TEA molecules per unit cell, the nascent AFI structure tends to incorporate a lower amount of organic SDA to enable a higher incorporation of water

molecules. Despite the better space filling achieved by only the occlusion of TEA molecules, the results indicate that the energetic balance between the water–AFI and SDA–AFI interactions favours the incorporation of a larger amount of water. The increased interaction energy reaches a maximum at ≈1.1 TEA molecules per unit cell, and is due not only to a higher water–AFI interaction but also to a high TEA–water interaction, owing to the hydrophilic nature of the TEA molecule (see Table 1 in the Supporting Information). The most thermodynamically stable situation corresponds to the simultaneous occlusion of 1.0–1.2 TEA molecules and around 9–10 water molecules per AFI unit cell, in close agreement with the experimental findings. Under these conditions, the SDA–AFI interaction represents only 50% of the total interaction energy, thus evidencing the important role that the occlusion of water molecules plays in making thermodynamically viable the crystallisation of the AFI structure under these conditions.

In the system with BP, two energy minima are found: at 1.33, which corresponds to the dimer configuration ("ss"), and at 1.0, in the "opp" configuration with simultaneous occlusion of water; however, a stable packing value of 0.66 is also found. This is again in good agreement with the experimental value of 1.00 BP molecules per unit cell. Except for the dimer configuration at high loading (1.33, "ss"), the most stable packing of the BP molecules is achieved in the "opp" configuration, which suggests that, although dimers might be present in the AFI structure, this molecule has a low probability to arrange as dimers (with benzyl rings of adjacent molecules interacting through π–π interactions), in agreement with our results from fluorescence studies.[27]

Interestingly, a different situation is found when the BPM molecule is used as the SDA. In this case we find a clear global minimum that corresponds to the highest loading of organic SDA molecules (organic content of 1.33 molecules per unit cell, in the dimer configuration "ss") and a much lower water occlusion (in fact, no water was loaded in the 12-MR channels, only four water molecules per unit cell in the 6-MR channels). This difference can be explained by the higher interaction that BPM develops with the AFI framework, owing to the presence of the methanol group that strongly interacts through H bonds with the oxide network; the SDA–AFI interaction increases by about 15 kcal mol^{-1} per unit cell as a result of functionalisation with the methanol group (Table 1 in the Supporting Information). Again, this result is in very good agreement with the experimental findings (1.23 BPM per unit cell). In this case, about 82% of the total interaction energy comes from the SDA–AFI interaction (the rest come from AFI–water interactions within the 6-MR channels). Energy results indicate that, at all loadings, the packing of the BPM molecules with benzyl rings facing each other is more stable, which suggests a preferential occlusion of the molecules as dimers, in contrast to the results found for BP and in good agreement with fluorescence results.[27]

Overall, the stable number of SDA and water molecules incorporated within the nascent microporous structure is a compromise between competing effects. The system can incorporate as much SDA as possible (this occurs when BPM is used as SDA) or it can incorporate a notable number of water molecules at the expense of the SDA content (when BP or TEA are used as SDAs). A competition between water and organic SDA molecules for occlusion within the AFI structure during its crystallisation is apparent: the equilibrium value depends on the net interaction of water and SDAs with the framework. When the SDA develops a strong interaction with the framework, as is the case for BPM due to the presence of the methanol group, the system tends to incorporate only the organic SDA. In contrast, when the interaction of the SDA with the framework is lower (TEA), the system incorporates both the organic SDA and water molecules, which increases the stabilisation through the development of strong electrostatic interactions in what could be considered as a cooperative structure-directing effect. When several energy minima are found for different SDA/water ratios (BP), competition between the organic SDA and water to be occluded within the AFI structure during crystallisation arises.

Interestingly, the stabilisation of the AFI structure achieved by the inclusion of only water molecules (−27.5 kcal mol^{-1}) is much lower than those with organic SDAs. This means that the occlusion of water molecules within the AFI structure does not provide enough stabilisation to direct the crystallisation of this large-pore structure; instead, denser phases (such as AlPO-C or trydimite) crystallise in synthesis gels where no organic molecules are present. Our results show that the presence of organic molecules is required in the synthesis gels for the AFI structure to be directed, and they exert a templating role that water cannot perform by itself: the presence of large organic molecules is required to template large-pore structures, maintain the open-framework structures and thus make viable the formation of the first nuclei.

It is worth mentioning here the anomalous trend we have found regarding the space-filling efficiency of the TEA system. It has long been recognised that one of the important issues to achieve structure direction is the space-filling role that the SDAs play during crystallisation of porous structures. However, our results demonstrate that the space-filling efficiency of the different water–TEA combinations is not the only factor governing the occlusion of the molecules within the microporous structure, because the best space-filling efficiency (two TEA molecules per unit cell, with a free volume of 408 Å^3) does not lead to the most stable system (one TEA and 6.5 water molecules per unit cell, with a free volume of 433 Å^3). The chemical nature of the interacting atoms (molecules) strongly influences the energetic balance of the systems. The space-filling effect of water is low due to its small molecular size, but its interaction is very high due to its strong dipole. The same can be argued for the alcohol group of the BPM molecule.

Water molecules seem to play another fundamental role in the crystallisation of the AFI structure. As previously shown, the water molecular size and geometry yield a good

match with the side 6-MR channels of AFI (Figure 5). The interaction energy between water in the 6-MR channels and the AFI framework accounts for as much as 15–20% of the total host–guest interaction energy, which indicates that water may have templating effects for a set of secondary building units, such as the 6-MR channels of the AFI framework. By itself, however, water is unable to stabilise microporous architectures.

The location of the water molecules within the 12-MR channels of the AFI structure, both when they are accompanying SDA molecules or if the 12-MR channels are exclusively loaded with water, is shown in Figure 8. We clearly

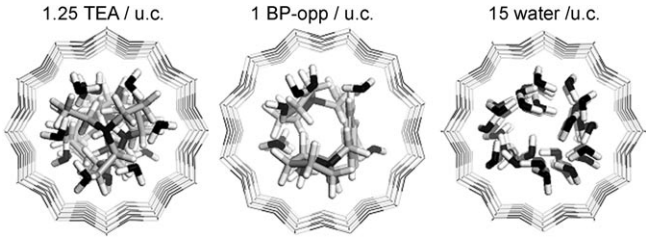

Figure 8. View (perpendicular to the channel direction) of the location of water and SDA molecules in the 12-MR channels in the most stable arrangements of the AFI structure loaded with TEA (left, 1 TEA and 10.5 water molecules per unit cell), BP (middle, 1 BP in the "opp" configuration and 9.3 water molecules per unit cell) and only water (right, 15 water molecules per unit cell in the 12-MR channel). N, O and C atoms are displayed in dark grey, black and light grey, respectively.

observe that in all cases the water molecules are located close to the channel walls, where they can establish H-bond interactions with the framework oxygen atoms, with the centre of the channel being filled by the core of organic SDA molecules or even being empty. This result suggests that functional groups susceptible to developing H bonds with the framework tend to locate, if the molecular geometry allows it, close to the channel walls to maximise the interaction. This finding could be useful for designing new and efficient SDA molecules for the synthesis of microporous aluminophosphates, in which a bulky organic core would be used to provide a large molecular size, and thus support the open-framework architecture of the microporous structures. A shell bearing strongly interacting groups, such as hydroxyl and/or amine groups, would provide the required interactions with the microporous network to stabilise the system and provide the required basicity.

Finally, we would like to stress the importance of the occlusion of water molecules inside hydrophilic microporous frameworks. Our energy results demonstrate that the presence of water molecules greatly stabilises the microporous structures and plays a key role during crystallisation of AlPO-type frameworks. In fact, $AlPO_4$-based networks, which are more hydrophilic in nature, are usually crystallised more easily than their SiO_2-based counterparts, with a more hydrophobic character; indeed, no water molecules are usually occluded within SiO_2-based structures. Therefore, the easier crystallisation of $AlPO_4$-based microporous structures could be at least partially explained by the water occlusion that takes place within these hydrophilic frameworks and the relative energetic stabilisation.

Conclusion

We have developed and applied a computational procedure that enables us to consider competition and cooperative effects in the structure direction of organic and water molecules in the synthesis of microporous aluminophosphates. The relative incorporation of the different species can be rationalised through their interaction energy with the framework.

Three different situations in the crystallisation of the AFI structure have been found. When the organic molecules interact strongly with the framework, as is the case for BPM, the crystallisation proceeds through the occlusion of the organic molecules within the 12-MR channel, whereas water molecules occupy the 6-MR channels and provide further stabilisation to the system through the development of strong electrostatic interactions. Instead, when the organic molecule interacts less strongly with the framework, as is the case for TEA, the system tends to incorporate simultaneously the bulky organic molecule and water molecules, thus providing the additional thermodynamic stabilisation required for the structure to be crystallised and representing a new example of a cooperative structure-directing effect. Finally, several minima for different SDA/water contents exist when BP is used as the SDA, which leads to competition between water and organic species for being occluded within the AFI structure.

The presence of a certain amount of organic SDA molecules is required in the synthesis gel to maintain the open-framework architecture of the AFI microporous structure; water by itself does not provide enough thermodynamic stabilisation to make viable the crystallisation of the large-pore AFI structure. This result indicates the importance of organic molecules as structure directors of large-pore frameworks, structurally holding the large-pore architectures.

Finally, it is worth mentioning that, although applied here to investigate the competition between water and organic SDAs, a similar computational procedure to the one that we employed could be applied to study co-templating in which the primary and secondary molecules are both organic.

Experimental Section

Experimental details: Details of the synthesis, purification and characterisation of the organic molecules employed in this study, BP and BPM, have been published earlier.[28,29] TEA was purchased from Sigma–Aldrich.

The syntheses of AlPO-5 by using the different molecules (TEA, BP or BPM) as SDAs were carried out in the following molar composition: 1 R:1 P_2O_5:1 Al_2O_3:40 H_2O, where R stands for the organic amine, which gave a pH in the 3–3.5 range. The respective gels were introduced into

60 mL Teflon-lined stainless-steel autoclaves and heated statically at 150 °C for 24 or 72 h. The resulting solids were separated by filtration, washed with ethanol and water and dried at 60 °C overnight.

Calcination of AlPO-5 samples was carried out by heating the sample at 500 °C under an inert atmosphere of N_2 for 1 h, followed by 5 h at the same temperature under an oxidant O_2 atmosphere. Complete removal of the organic molecule was assessed by TGA.

The crystallisation of the AFI structure as a pure phase was assessed by XRD (Seifert XRD 3000P diffractometer, CuKα radiation). The organic content of the samples was studied by chemical CHN analysis (Perkin–Elmer 2400 CHN analyser) and TGA carried out in air (Perkin–Elmer TGA7 instrument). The number of organic molecules per unit cell of the AFI framework in the different samples was calculated by relating the organic content (obtained from the elemental analyses) to the percentage of inorganic material (weight percentage of sample remaining at the end of the TGA). To be able to quantitatively measure the amount of water occluded in the solids, the samples were kept, prior to the TGA, under an atmosphere with a controlled humidity of about 33% (given by a $MgCl_2{\cdot}6H_2O$ saturated solution kept at room temperature) for 24 h. The water content per unit cell of the AFI framework was obtained from the weight loss observed in the TGA, by subtracting from the total weight loss the one corresponding to the organic molecules (known by elemental analysis) and the one corresponding to framework dehydroxylation processes. The latter value was calculated as the weight loss in the 200–900 °C temperature range of the calcined AlPO-5 sample, the temperature range at which water release had ended and no organic molecule remained in the solid after calcination (see Figure 2 in the Supporting Information).

TGA studies were also performed coupled with mass spectrometry for analysing the evolved gas (Fisons MD-800 mass spectrometer, with an ionisation potential of 70 eV, a 6 scan/min frequency and an atomic mass range of 2–200 a.m.u.). In this case, TGA was carried out under a helium atmosphere. Mass spectra taken at temperatures when the main desorption came from the organic molecules indicated that the main *m*/*z* value for TEA was 86, which corresponded to the $(CH_3CH_2)_2NCH_2^+$ ion, after loss of a terminal methyl group, whereas that for BP and BPM was 91, which corresponded to the benzyl moiety ($PhCH_2^+$, as the tropilium cation). In the TGA–mass spectrometry experiments, the release of water as a function of temperature was monitored by following the presence in the evolved gas of *m*/z 18, while desorption of the organic TEA, BP and BPM was monitored by following the *m*/*z* of 86, 91 and 91, respectively.

Computational details: Molecular structures and the interaction energies of the SDAs and water with the AFI framework were described with the consistent valence force field (CVFF).[30] This force field was originally developed for small organic molecules but has been developed for materials science applications, including the simulation of zeolite and related structures, to which it has been successfully applied recently.[21–23,31–33] The AFI framework atoms were kept fixed during all the calculations. Due to the very acidic pH of the synthesis gels (3–3.5), SDA molecules are expected to be protonated during the crystallisation of the AFI structure; therefore, protonated TEA, BP and BPM ammonium cations were studied. The atomic charges for these organic ammonium cations (total molecular charge of +1) were calculated by the charge-equilibration method.[34] The net molecular charge of +1 had to be compensated by the inorganic AFI framework; we employed a charge-balance model in which charged SDAs are compensated by a uniform distribution of charge across the whole structure,[35] obtained by decreasing the atomic charge for every Al and P framework ion until charge neutrality was achieved. The atomic charges for the water molecules were −0.82 and +0.41 for oxygen and hydrogen, respectively; this charge distribution has been shown to describe well the properties of water-containing systems.[32]

The simulated annealing calculations consisted of heating the system from 300 to 700 K with temperature increments of 10 K, and then cooling to 300 K again in the same way. Five hundred MD steps of 1.0 fs (for a total of 0.5 ps) were run in every heating/cooling step. At the end of each cycle the system was geometry optimised.

Free volumes were calculated from van der Waals surfaces, by using a grid interval of 0.75 Å and a van der Waals factor of 1. The free volume of the empty AFI structure is 717 $Å^3$ per unit cell, whereas the volume of a water molecule is 18 $Å^3$.

Acknowledgements

Financial support by the Spanish Ministry of Education and Science (project CTQ2006-06282) is acknowledged. L.G.-H. acknowledges the Spanish Ministry of Education and Science for a postdoctoral grant; F.C. is supported by an RCUK Fellowship. The authors also thank Accelrys for providing their software, and Centro Técnico de Informática for running some of the calculations.

[1] M. E. Davis, *Acc. Chem. Res.* **1993**, *26*, 111–115.
[2] J. E. Naber, K. P. de Jong, W. H. J. Stork, H. P. C. E. Kuipers, M. F. M. Post, *Stud. Surf. Sci. Catal.* **1994**, *84*, 2197–2219.
[3] P. B. Venuto, *Microporous Mater.* **1994**, 2, 297–411.
[4] S. T. Wilson, B. M. Lok, E. M. Flanigen, US Patent, 4310440, **1982**.
[5] http://www.iza-structure.org/databases
[6] B. M. Lok, T. R. Cannan, C. A. Messina, *Zeolites* **1983**, *3*, 282–291.
[7] M. E. Davis, R. F. Lobo, *Chem. Mater.* **1992**, *4*, 756–768.
[8] S. I. Zones, Y. Nakagawa, G. S. Lee, C. Y. Chen, L. T. Yuen, *Microporous Mesoporous Mater.* **1998**, *21*, 199–211.
[9] H. Gies, B. Marler, *Zeolites* **1992**, *12*, 42–49.
[10] S. Caratzoulas, D. Vlachos, M. Tsapatsis, *J. Phys. Chem. B* **2005**, *109*, 10429–10434.
[11] S. Caratzoulas, D. Vlachos, M. Tsapatsis, *J. Am. Chem. Soc.* **2006**, *128*, 596–606.
[12] S. Caratzoulas, D. Vlachos, M. Tsapatsis, *J. Am. Chem. Soc.* **2006**, *128*, 16138–16147.
[13] S. Caratzoulas, D. Vlachos, *J. Phys. Chem. B* **2008**, *112*, 7–10.
[14] M. E. Davis, C. Montes, P. E. Hathaway, J. P. Arhancet, D. L. Hasta, J. M. Garces, *J. Am. Chem. Soc.* **1989**, *111*, 3919–3924.
[15] P. B. Malla, S. Komarneni, *Zeolite* **1995**, *15*, 324–332.
[16] B. L. Newalkar, R. V. Jasra, V. Kamath, S. G. T. Bhat, *Microporous Mesoporous Mater.* **1998**, *20*, 129–137.
[17] N. Floquet, J. P. Coulomb, N. Dufau, G. Andre, *J. Phys. Chem. B* **2004**, *108*, 13107–13115.
[18] L. B. McCusker, C. Baerlocher, E. Jahn, M. Bülow, *Zeolites* **1991**, *11*, 308–313.
[19] E. Fois, A. Gamba, A. Tilocca, *J. Phys. Chem. B* **2002**, *106*, 4806–4812.
[20] *CRC Handbook of Chemistry and Physics*, 75th ed. (Ed.: D. R. Lide), CRC Press, Boca Raton **1994**.
[21] L. Gómez-Hortigüela, F. Corà, C. R. A. Catlow, J. Pérez-Pariente, *J. Am. Chem. Soc.* **2004**, *126*, 12097–12102.
[22] L. Gómez-Hortigüela, J. Pérez-Pariente, F. Corà, C. R. A. Catlow, T. Blasco, *J. Phys. Chem. B* **2005**, *109*, 21539–21548.
[23] L. Gómez-Hortigüela, F. Corà, C. R. A. Catlow, J. Pérez-Pariente, *Phys. Chem. Chem. Phys.* **2006**, *8*, 486–493.
[24] G. J. Klap, S. M. van Klooster, M. Wübbenhorst, J. C. Hansen, H. van Bekkum, J. van Turnhout, *J. Phys. Chem. B* **1998**, *102*, 9518–9524.
[25] G. J. Klap, M. Wübbenhorst, J. C. Hansen, H. van Koningsveld, H. van Bekkum, J. van Turnhout, *J. Mater. Chem.* **1999**, *11*, 3497–3503.
[26] G. J. Klap, H. van Koningsveld, H. Graafsma, A. M. M. Schreurs, *Microporous Mesoporous Mater.* **2000**, *38*, 403–412.
[27] L. Gómez-Hortigüela, F. López-Arbeloa, F. Corà, J. Pérez-Pariente, *J. Am. Chem. Soc.* **2008**, *130*, 13274–13284.
[28] L. Gómez-Hortigüela, J. Pérez-Pariente, T. Blasco, *Microporous Mesoporous Mater.* **2005**, *78*, 189–197.
[29] L. Gómez-Hortigüela, J. Pérez-Pariente, T. Blasco, *Microporous Mesoporous Mater.* **2007**, *100*, 55–62.

[30] P. Dauger-Osguthorpe, V. A. Roberts, D. J. Osguthorpe, J. Wolff, M. Genest, A. T. Hagler, *Proteins Struct. Funct. Genet.* **1988**, *4*, 31–47.
[31] E. C. Moloy, R. T. Cygan, F. Bonhomme, D. M. Teter, A. Navrotsky, *Chem. Mater.* **2004**, *16*, 2121–2133.
[32] J. J. Williams, C. W. Smith, K. E. Evans, Z. A. D. Lethbridge, R. I. Walton, *Chem. Mater.* **2007**, *19*, 2423–2434.
[33] R. Garcia, E. F. Philp, A. M. Z. Slawin, P. A. Wright, P. A. Cox, *J. Mater. Chem.* **2001**, *11*, 1421–1427.
[34] A. K. Rappe, W. A. Goddard III, *J. Phys. Chem.* **1991**, *95*, 3358–3363.
[35] L. Gómez-Hortigüela, F. Corà, C. R. A. Catlow, T. Blasco, J. Pérez-Pariente, *Stud. Surf. Sci. Catal.* **2005**, *158*, 327–334.

Received: July 18, 2008
Revised: October 16, 2008
Published online: December 29, 2008

